JOURNAL OF MAGNETIC RESONANCE, Series A **101**, 30–40 (1993)

Spin-Echo Behavior of Nonintegral-Spin Quadrupolar Nuclei in Inorganic Solids*

JÜRGEN HAASE†‡§ AND ERIC OLDFIELD†

†*Department of Chemistry, University of Illinois at Urbana–Champaign, 505 South Mathews Avenue, Urbana, Illinois 61801; and* ‡*Sektion Physik der Universität Leipzig, Linnéstrasse 5, Leipzig, Germany*

Received December 19, 1991; revised March 26, 1992

The response to spin-echo radiofrequency pulse excitation of a variety of nonintegral-spin quadrupolar nuclei (^{23}Na, ^{27}Al, and ^{93}Nb) in inorganic solids (single-crystal ruby and sapphire, α-Al_2O_3, γ-Al_2O_3, AlN, $NaNO_3$, $KNbO_3$, $NaNbO_3$, $LiNbO_3$, albite, and the zeolite Linde A), subject to strong quadrupolar interactions and dipolar interactions of varying strength, is reported. It is demonstrated that "soft" RF pulse excitation with a pair of selective $\pi/2$ and π pulses yields predictable spin-echo decay behavior as a function of dipolar interaction, the experimental results being in good agreement with the theoretical predictions.

INTRODUCTION

In the past few years, there has been a rapid growth in the area of NMR studies of nonintegral-spin quadrupolar nuclei (e.g., ^{17}O, ^{27}Al) in various inorganic solids—such as zeolites, glasses, ceramics and minerals (*1*). Most studies have concentrated on measurement of isotropic chemical shifts, δ_i, and, to some extent, nuclear quadrupole coupling constants (e^2qQ/h) and have made a range of correlations between these parameters and various structural features—such as bond angles and coordination number. To date, however, there have been relatively few studies of linewidths and spin–spin (spin-echo decay) and spin–lattice relaxation in such materials. In this paper, we discuss the linewidths and spin–spin relaxation behavior of a variety of nonintegral-spin quadrupolar nuclei in solids, and elsewhere we report on a multinuclear NMR study of spin–lattice relaxation in a series of zeolites (*2*).

These topics are of importance since they provide new insight into the static and dynamic structure of solids—including (in principle) amorphous materials. In a recent letter, Han and Kessemeier (*3*) discussed the spin-echo decay behavior of a Si(B) semiconductor, but did not incorporate dipolar interactions. Similarly, Dolinsek (*4*) reported, using a two-dimensional technique, the spin-echo decay behavior of a glass, but again did not provide a quantitative theory to interpret the results. In this paper, we provide the first quantitative theory of spin-echo decay behavior in the presence of dipolar interactions, and we test the theory by using results obtained on a wide range of materials of general chemical, geochemical, and materials science interest (such as aluminas, perovskites, and zeolites). Such studies should provide a theoretical basis for testing models of, e.g., semiconductor (*3*) or glass (*4*) structure.

EXPERIMENTAL

NMR aspects. NMR measurements were performed on "homebuilt" NMR spectrometers, which operate at 8.45 or 11.7 T and use Oxford Instruments (Osney Mead, UK) superconducting solenoids, together with Nicolet (Madison, Wisconsin) model 1280 computer systems and Henry Radio (Los Angeles, California) Model 1002 and Amplifier Research (Souderton, Pennsylvania) Model 150LA or 200L radiofrequency amplifiers. The sample size was typically one-half the length of the RF coil, in order to minimize RF field inhomogeneity effects. The RF amplification was initially varied to determine the strongest pulse yielding an almost sinusoidal dependence of the intensity of the central line on the pulse length, as a proof of selective excitation (*5*). For the echo measurements, a pulse program of two in-phase pulses was used, combined with a standard CYCLOPS phase cycling (*6*). Data acquisition started at time Δ (the pulse separation) after the second pulse. The area under the Fourier-transformed lineshape was used as a measure of the echo intensity. The recycle time was always chosen after determination of the spin–lattice relaxation time, T_1, in order to exclude saturation effects.

Chemical aspects. Ruby laser rods (Cr^{3+} dopant level ~0.05%) were purchased from General Ruby and Sapphire Corp. (New Port Richey, Florida). Dr. R. J. Kirkpatrick (University of Illinois at Urbana–Champaign) provided the

* This work was supported by the Solid State Chemistry Program of the U.S. National Science Foundation (Grant DMR 88-14789) and by the Materials Research Laboratory Program (Grant DMR 89-20538).

§ Stipendiat of the Deutsche Forschungsgemeinschaft.

1064-1858/93 $5.00

mineral albite. Corundum powder was from Fisher Scientific (Fair Lawn, New Jersey), and γ-Al_2O_3 was from Alfa Products (Danvers, Massachusetts). Two AlN samples [AlN(1), AlN(2)] were provided by VEB Kombinat Keramische Werke Hermsdorf (*7*) while a third sample [AlN(3); 98% purity] was purchased from Aesar (Seabrook, New Hampshire). $NaNO_3$ was from Mallinckrodt (St. Louis, Missouri). $NaNbO_3$ and $LiNbO_3$ powders (99.9%) were purchased from CERAC (Milwaukee, Wisconsin). NaA zeolite was the gift of Dr. E. Flanigen (Union Carbide Corp., Tarrytown, New York). The $Na_{3.2}Ca_{4.4}A$ sample, Zeosorb 5AZ, was purchased from VEB Chemiekombinat (Bitterfeld, Germany).

THEORETICAL CONSIDERATIONS

A situation often met with in NMR studies of powdered inorganic solids (*8*) can be represented by the equation

$$\|\mathcal{H}_Z\| \gg \|\mathcal{H}_Q\| \gg \|\mathcal{H}_D\| \approx \|\mathcal{H}_Q^{(2)}\|, \qquad [1]$$

where $\mathcal{H}_Z$ is the Zeeman interaction, $\mathcal{H}_Q$ the quadrupolar interaction, $\mathcal{H}_D$ the dipolar interaction, and $\mathcal{H}_Q^{(2)}$ the second-order quadrupolar interaction. In general, the first-order term of the quadrupolar interaction, $\mathcal{H}_Q^{(1)}$, overwhelmingly dominates the homonuclear and heteronuclear dipolar interactions, $\mathcal{H}_D$, while the second-order quadrupolar interaction, $\mathcal{H}_Q^{(2)}$, is about as important as the dipolar interactions. The effect of dipolar coupling on the central transition in terms of the second moment is well known and has been treated theoretically by Kambe and Ollom (*9*) and by Mansfield (*10*). The expressions for the corresponding second moments can be summarized by Van Vleck's formula for identical spins as [cf. Abragam (*11*, pp. 129–130)]

$$M_{2F} = F(I)\gamma^4\hbar^2 \sum_j b_{ij}^2$$

$$= F(I)\gamma^4\hbar^2 \sum_j \left[\frac{3}{2}\frac{1 - 3\cos^2\theta_{ij}}{r_{ij}^3}\right]^2, \qquad [2]$$

where

$$F(I) = \frac{I(I+1)}{3}. \qquad [3]$$

Equation [3] together with Eq. [2] describes the second moment due to homonuclear dipolar interactions in the absence of a quadrupolar coupling. It has been shown (*9–11*) that in the presence of a quadrupolar coupling, the second moment of the *central transition* due to homonuclear dipolar interactions can be described by Eq. [2] by introducing different factors $F(I)$. If all spins are subjected to the same quadrupolar coupling (same magnitude and orientation of the electric field gradient), the spins have been called "like spins" and the corresponding factor, $F(I) = F_L$, is given by

$$F_L = \frac{4I(I+1)}{27} + \frac{\{2I^2(I+1)^2 + 3I(I+1) + 13/8\}}{18(2I+1)}. \qquad [4]$$

However, if the quadrupolar coupling of the two spins is different, but the central transition frequencies are still the same, the spins may be called "semi-like spins" and the corresponding factor, $F(I) = F_{SL}$, is given by

$$F_{SL}(I) \equiv F_{SL} = \frac{1}{9}\left\{\frac{4I(I+1)}{3} + \frac{(2I+1)}{2} + \frac{(2I+1)^3}{32}\right\}. \qquad [5]$$

Comparison of these factors shows that they are the same, within about ±20%, and are thus relatively unimportant with respect to linewidth analyses. We now consider the effects of these dipolar interactions on the spin-echo decay.

Using the interaction representation, transformed by the Zeeman interaction, we can describe in superoperator notation (*12*) the intensity of an echo occurring at times 2Δ (as indicated in Fig. 1A) by the trace

$$E(2\Delta) = \mathrm{tr}\{\rho(2\Delta)I_+\} \equiv (I_-|\rho(2\Delta)), \qquad [6]$$

where

$$|\rho(2\Delta)) = \exp\{-i\mathcal{H}\Delta\}\exp\{-i\mathcal{P}_2\tau_2\} \times \exp\{-i\mathcal{H}\Delta\}\exp\{-i\mathcal{P}_1\tau_1\}|\rho_0). \qquad [7]$$

For convenience, we use the transformation

$$\mathcal{H}_r = \exp\{-i\mathcal{P}_2\tau_2\}\mathcal{H}\exp\{i\mathcal{P}_2\tau_2\} \qquad [8]$$

and can then write

$$|\rho(2\Delta)) = \exp\{-i\mathcal{H}\Delta\}\exp\{-i\mathcal{H}_r\Delta\} \times \exp\{-i\mathcal{P}_2\tau_2\}\exp\{-i\mathcal{P}_1\tau_1\}|\rho_0), \qquad [9]$$

where the Hamiltonians $\mathcal{P}_1$ ($\mathcal{P}_2$) and $\mathcal{H}$, all expressed in the interaction representation, describe the interactions during the first (second) pulse and in the absence of RF excitation, respectively, and they may be approximated by means of the Magnus expansion (*13*) as

$$\mathcal{H} = \bar{\mathcal{H}}_Q^{(1)} + \bar{\mathcal{H}}_Q^{(2)} + \bar{\mathcal{H}}_D^{(1)};$$
$$\mathcal{P}_{1(2)} = \bar{\mathcal{H}}_{RF\,1(2)}^{(1)} + \bar{\mathcal{H}}_Q^{(1)}. \qquad [10]$$

Since the quadrupolar interaction dominates, and the interaction of the spins with the RF field, $\mathcal{H}_{RF}$, is assumed to exceed second-order quadrupolar contributions as well as the dipolar interactions amongst the spins, we retain during the RF excitation only the first-order quadrupolar term, $\bar{\mathcal{H}}_Q^{(1)}$, and the first-order part of the RF excitation, $\bar{\mathcal{H}}_{RF}^{(1)}$. In the absence of RF excitation, we consider the quadrupolar effects in first order, as well as in second order, $\bar{\mathcal{H}}_Q^{(1)} + \bar{\mathcal{H}}_Q^{(2)}$, and the dipolar interaction in first order, $\bar{\mathcal{H}}_D^{(1)}$. Finally, in the high-temperature approximation, we have

$$|\rho_0) \sim \sum_j |I_z^j). \qquad [11]$$

Now, in order to determine the spin-echo decay behavior, we calculate the second moment, M_{2E}, of the envelope of a train of echoes, as

$$M_{2E} = -\frac{d^2}{d(2\Delta)^2} E(2\Delta)\Big|_{2\Delta=0}. \qquad [12]$$

We find, introducing Eqs. [6]–[9] into Eq. [12], that

$$M_{2E} = (1/4)\{(I_-|[\mathcal{H}, [\mathcal{H}, \rho_1]]) + 2(I_-|[\mathcal{H}, [\mathcal{H}_r, \rho_1]]) + (I_-|[\mathcal{H}_r, [\mathcal{H}_r, \rho_1]])\}, \qquad [13]$$

where

$$|\rho_1) = \exp\{-i\mathcal{P}_2\tau_2\}\exp\{-i\mathcal{P}_1\tau_1\}|\rho_0). \qquad [14]$$

We consider first the case of a purely homonuclear dipolar coupling between like spins (i.e., all spins are subject to the same quadrupolar coupling) on the spin-echo decay of the central transition and neglect second-order quadrupolar effects, i.e. $\|\bar{\mathcal{H}}_Q^{(2)}\| \ll \|\bar{\mathcal{H}}_D^{(1)}\|$. The first-order quadrupolar interaction is given by the expression

$$\bar{\mathcal{H}}_Q^{(1)} = \frac{\omega_{Q'}}{6}[3I_z^2 - I(I+1)] \qquad [15]$$

where

$$\omega_{Q'} = \frac{\omega_Q}{2}(3\cos^2\beta - 1 + \eta\sin^2\beta\cos 2\alpha), \qquad [16]$$

and

$$\nu_Q = \frac{\omega_Q}{2\pi} = \frac{3e^2qQ}{h2I(2I-1)}. \qquad [17]$$

The quantities in Eqs. [15]–[17] have their usual meanings, with α and β denoting the azimuthal and polar angle of the electric field gradient tensor in the laboratory-axis system, respectively.

We will demonstrate the calculation of the second moment of the spin-echo decay by using selective excitation with an in-phase pulse pair, that is, a "Hahn" echo sequence using selective $\pi/2$ and selective π pulses, where a selective π pulse means that, first

$$2W_m\omega_{RF}\tau = \pi, \qquad [18]$$

with

$$W_m = (1/2)\sqrt{I(I+1) - m(m+1)}. \qquad [19]$$

Second, the bandwidth of excitation, which is about $2/\pi\tau$ for a pulse of duration τ, is not much larger than the linewidth of the transition under investigation. Thus, we have for $\mathcal{P}_1$ and $\mathcal{P}_2$, Eq. [14], for selective excitation of the central transition, and assuming y pulses,

$$\mathcal{P}_1 = \frac{\pi}{2(I+1/2)}I_y + \bar{\mathcal{H}}_Q^{(1)};$$

$$\mathcal{P}_2 = \frac{\pi}{(I+1/2)}I_y + \bar{\mathcal{H}}_Q^{(1)}. \qquad [20]$$

Now, since we are assuming selective excitation of the central transition, the echo sequence can be interpreted as a result of an initially applied $3\pi/2$ pulse (cf. Eq. [14]), and the following propagation of the density operator: first, by the operator $\mathcal{H}_r$ for a time interval Δ, second, by the operator $\mathcal{H}$ for the time interval Δ (cf. Eq. [9]). This selective $3\pi/2$ pulse changes only the diagonal elements of the equilibrium density operator ($\rho_0 = I_z$) corresponding to the central levels into I_x components, while leaving the diagonal elements (for $|m| > 1/2$) unchanged (*10*). So, ρ_1 has only nonvanishing I_x components for $|m| = 1/2$. From this it can be seen that ρ_1 commutes with $\bar{\mathcal{H}}_Q^{(1)}$, $[\bar{\mathcal{H}}_Q^{(1)}, \rho_1] = 0$. The selective π pulse, which must be used for the transformation in Eq. [8], exchanges only, for a diagonal matrix, the elements corresponding to the central transition. Thus, since $\bar{\mathcal{H}}_Q^{(1)}$ is symmetric in the main diagonal, we find from Eq. [8] that $\bar{\mathcal{H}}_{Qr}^{(1)} \equiv \bar{\mathcal{H}}_Q^{(1)}$. For a homonuclear dipolar interaction we consider the Hamiltonian for two spins, as reported previously by Mansfield (*10*). Restriction to the first-order term yields

$$\bar{\mathcal{H}}_D^{(1)} = -aI_zI_z' + \frac{a}{4}(I_+I_-' + I_+'I_-), \qquad [21]$$

which is secular with respect to $(I_z + I'_z)$ and $(I_z^2 + I_z'^2)$, the Zeeman and first-order quadrupolar terms for two like spins. Since $\bar{\mathscr{H}}_{Qr}^{(1)} \equiv \bar{\mathscr{H}}_{Q}^{(1)}$, $[\bar{\mathscr{H}}_{Q}^{(1)}, \bar{\mathscr{H}}_{D}^{(1)}] = 0$, and $[\bar{\mathscr{H}}_{Q}^{(1)}, \rho_1] = 0$, we have to calculate only the expressions in Eq. [13] for $\mathscr{H} = \bar{\mathscr{H}}_{D}^{(1)}$ and $\mathscr{H}_r \equiv \bar{\mathscr{H}}_{Dr}^{(1)}$, where $\bar{\mathscr{H}}_{Dr}^{(1)}$ follows from Eq. [8] and is given by

$$\bar{\mathscr{H}}_{Dr}^{(1)} = \exp\{-i\mathscr{P}_2\tau_2\}\bar{\mathscr{H}}_{D}^{(1)}\exp\{i\mathscr{P}_2\tau_2\}. \quad [22]$$

From the matrix elements of $\bar{\mathscr{H}}_{D}^{(1)}$ and $\bar{\mathscr{H}}_{Dr}^{(1)}$, necessary to calculate the traces in Eq. [13], we retain the following elements [see also Ref. (11, p. 129) and Ref. (*10*)]: the diagonal terms $(m, m'|\bar{\mathscr{H}}_{D}^{(1)}|m, m')$, $(m, m'|\bar{\mathscr{H}}_{Dr}^{(1)}|m, m')$, and the off-diagonal terms $(m \pm 1, m|\bar{\mathscr{H}}_{D}^{(1)}|m, m \pm 1)$ and $(m \pm 1, m|\bar{\mathscr{H}}_{Dr}^{(1)}|m, m \pm 1)$. Since we are exciting and observing a single transition only, the matrix elements of I_+ are required to correspond to transitions between the central levels, i.e., $(m, +1/2|I_+|m, -1/2)$ and $(+1/2, m'|I_+|-1/2, m')$ (*10, 11*).

For the calculation of the matrix elements of the transformed dipolar Hamiltonian, $\bar{\mathscr{H}}_{Dr}^{(1)}$, we now need to consider two cases: First, if only the excited levels are involved, we can view $\bar{\mathscr{H}}_{Dr}^{(1)}$ as being transformed by a nonselective pulse:

$$\bar{\mathscr{H}}_{Dr}^{(1)} = \exp\{i\pi(I_y + I'_y)\}\bar{\mathscr{H}}_{D}^{(1)}\exp\{-i\pi(I_y + I'_y)\}$$

and

$$\bar{\mathscr{H}}_{Dr}^{(1)} = \bar{\mathscr{H}}_{D}^{(1)} = -aI_zI'_z + \frac{a}{4}(I_+I'_- + I'_+I_-). \quad [23]$$

For matrix elements relating the two Zeeman levels of the excited transition of one of the two spins to different spin states of the other spin, i.e., the Zeeman levels are not affected by the excitation, a selective pulse acts only on the spins in the excited levels, and the transformation, given by Eq. [22], yields the Hamiltonian

$$\bar{\mathscr{H}}_{Dr}^{(1)} = +aI_zI'_z - \frac{a}{2}I_xI'_x + \frac{a}{2}I'_yI_y. \quad [24]$$

Summing up the appropriate matrix elements gives the expressions for the second moment of the envelope of the Hahn-echo train, M_{2E}. In analogy to Eq. [2], we define M_{2E} as

$$M_{2E} = E_L^{(n)}\gamma^4\hbar^2\sum_j b_{ij}^2, \quad [25]$$

where $E_L^{(n)}$ is a spin-dependent factor, "L" refers to "like spins," and the label $n = 0, 1, \cdots [n < (I + 1/2)]$ denotes the central transition and the first satellite transitions, respectively. For the central transition, we find

$$E_L^{(0)} = \frac{2}{9(2I+1)}(1 + 4W^2_{-1/2} + 4W^4_{-1/2} + W^4_{+1/2}), \quad [26]$$

where the W_m are defined in Eq. [19]. We prefer to use the notation given in Eq. [26] since it reveals directly the transitions in the spin system: "1" represents the diagonal contribution of the central levels, i.e., neither spin changes its quantum number, due to $\bar{\mathscr{H}}_{D}^{(1)}$, until the echo forms. $W^2_{-1/2}$ represents transitions where, until application of the first pulse, spin flipping occurs between the central levels, and between the first pulse and the echo there is no change; $W^4_{-1/2}$ stands for flip-flops during both time periods; and, finally, $W^4_{+1/2}$ stands for flip-flops in the transitions next to the central one $(\pm 3/2)$ during both time periods.

In the notation of Eq. [26], F_L in Eq. [4] can be recast as

$$F_L = \frac{2}{9(2I+1)} \times (2\sum_{m=-I}^{I} m^2 + 4W^2_{-1/2} + 4W^4_{-1/2} + 4W^4_{+1/2}). \quad [27]$$

Comparison with Eq. [26] shows that, except for terms with $m = \pm 1/2$, the diagonal contribution cancels for the echo; i.e., spins with $|m| > 1/2$ which do not flip until the echo forms do not contribute to the echo decay. Also, the flip-flop term between the levels next to the central ones is reduced by a factor of 4, but its contribution in both Eq. [26] and Eq. [27] is negligible. Inserting spin quantum numbers, we obtain the ratios between the ordinary second moment of the central transition for like spins and the second moment of the spin-echo decay $(F_L^{(0)}/E_L^{(0)})$ given in Table 1. As may be seen from these results, the ratios are essentially independent of the spin-quantum number, I. As might have been anticipated, the Hahn spin-echo decay behavior of the "isolated" central transition is mainly governed by the di-

TABLE 1

Ratio between the Second Moment of the Fourier Transform of the Envelope of the Echo Decay and the Ordinary Second Moment, for Homonuclear Dipolar Interactions and Various Spin Quantum Numbers, I

	$I = 3/2$	$I = 5/2$	$I = 7/2$	$I = 9/2$
$E_L{}^a/F_L{}^b$	0.455	0.427	0.431	0.446
$\sqrt{F_L/E_L}$	1.48	1.53	1.52	1.50

[a] E_L corresponds to the second moment of the Fourier transform of the envelope of the spin-echo decay.

[b] F_L corresponds to the ordinary second moment, for a homonuclear dipolar interaction. From Eqs. [26] and [27] in the text.

polar interactions between the fraction of spins having magnetic quantum numbers of $m = \pm 1/2$.

If like spins experience a slightly different quadrupolar coupling, i.e., the first-order quadrupolar interactions are different [such spins have also been called "semi-like" spins; cf. Ref. (*11*, p. 130)], their central transition frequencies are still the same, but the satellite transition frequencies can be very different. In this case it can be concluded from the above analysis that the spin-echo decay for the central transition will not be changed unless there is an additional frequency shift for the central transition as well, due for example to a chemical-shift nonequivalence.

Satellite transitions. For a single crystal, satellite transitions can usually be observed. We have calculated the second moments given below (in terms of Eqs. [4] and [26]), for each of the satellites for a single-pulse experiment, as well as for the echo envelopes, and found the following:
For the first satellites (for $I = 5/2$),

$$F_L^{(1)} = \frac{2}{9(2I+1)}\left(2\sum_{m=-I}^{I} m^2 + 4W_{+1/2}^2 + 4W_{+1/2}^4 + 2W_{-1/2}^4 + 2W_{+3/2}^4\right) \quad [28]$$

$$E_L^{(1)} = \frac{2}{9(2I+1)}\left(5 + 4W_{+1/2}^2 + 4W_{+1/2}^4 + \frac{1}{2}W_{-1/2}^4 + \frac{1}{2}W_{+3/2}^4\right). \quad [29]$$

For the second satellites (for $I = 5/2$),

$$F_L^{(2)} = \frac{2}{9(2I+1)} \times \left(2\sum_{m=-I}^{I} m^2 + 4W_{+3/2}^2 + 4W_{+3/2}^4 + 2W_{+1/2}^4\right) \quad [30]$$

$$E_L^{(2)} = \frac{2}{9(2I+1)} \times \left(14 + 4W_{+3/2}^2 + 4W_{+3/2}^4 + \frac{1}{2}W_{+1/2}^4\right). \quad [31]$$

For $I = 5/2$, the intensity ratios are

$$\frac{F_L}{E_L} = \frac{321}{137}; \quad \frac{F_L^{(1)}}{E_L^{(1)}} = \frac{289}{512/4}; \quad \frac{F_L^{(2)}}{E_L^{(2)}} = \frac{217}{121}. \quad [32]$$

The above results for the spin-echo decay of the satellite transitions apply only to like spins. For semi-like spins, the spin-echo decay of the satellite transitions can be slowed down considerably because even slight differences in the quadrupolar couplings of neighboring spins (which do not affect the central transition) can cause great differences in the satellite transition frequencies, and spin exchange is no longer effective.

If *second-order quadrupolar effects* are present, $\bar{\mathcal{H}}_Q^{(2)}$ must be considered as well, and unfortunately analytical expressions for $\bar{\mathcal{H}}_Q^{(2)}$ are rather lengthy. However, when considering a given transition, $\bar{\mathcal{H}}_Q^{(2)}$ can be viewed as a fictitious spin-1/2 operator, in which case we have $\bar{\mathcal{H}}_Q^{(2)} = \Omega\sigma_z$, where Ω is the orientation-dependent second-order frequency shift, and σ_z denotes the z component of the spin-angular momentum operator for $I = 1/2$. Since a selective π pulse converts σ_z into $-\sigma_z$, it can be seen from Eq. [13] that, for a Hahn-echo sequence, the second-order quadrupolar interaction is greatly reduced, as in the case of a resonance offset effect. Clearly, this is only a qualitative description of the influence of the second-order quadrupolar interaction, and its part which does not commute with the first-order interaction may govern the spin-echo decay if no dipolar interactions are present (*3*). However, as long as the Zeeman levels represent stable states within the time scale of the formation of the spin echo, the influence of the second-order quadrupolar interactions can be neglected when using a selective $\pi/2$—π pulse sequence.

The effect of a 90° phase shift between the $\pi/2$ and the π pulse can be calculated by using an x pulse instead of a y pulse for the first $\pi/2$ pulse. In this case, as long as a selective excitation is guaranteed, ρ_1 in Eq. [14] contains I_y components for $m = \pm 1/2$ and is diagonal for $|m| > 1/2$, as before, and the spin-echo decay will not change, except that the echo is now in-phase with the one-pulse free-induction decay.

For a selective $(\pi/2)_x$—$(\pi/2)_y$ pulse sequence, we calculate the same numbers for $E_L^{(0)}$, within about 10% (neglecting second-order quadrupolar effects). These results have been proven experimentally by measurements on single crystals. However, since the second pulse is now a $\pi/2$ pulse, it does not reduce the second-order quadrupolar interaction as is the case with a π pulse. Also, resonance offset effects are not eliminated. Especially for powders, with a large spread in second-order frequency shifts, or a chemical-shift anisotropy, a faster echo decay is observed experimentally. This effect can even dominate with slowly decaying echoes, as found, for example, with several zeolites having low Al content (see below).

Reduced second moments. As was shown by Kambe and Ollom (*9*) and by Mansfield (*10*), the frequency shift due to the first-order quadrupolar interaction restricts spin exchange to the same transition of neighboring nuclei. This is why, for calculation of the second moment of the central transition, only the matrix elements of the homonuclear dipolar interaction (which are diagonal or describe the spin flipping between the same transitions) must be added. We have also seen for a $\pi/2$—π pulse sequence that the spin-echo decay of the central transition is overwhelmingly dom-

inated by the dipolar interactions of the spins populating the Zeeman levels with $m = \pm 1/2$. Therefore, it should be possible to describe the spin-echo decay of the central transition by its ordinary second moment for the one-pulse response, where we discard for the sum of the dipolar matrix elements all those elements which involve Zeeman levels for which $|m| > 1/2$. We thereby calculate a *reduced* second moment, characterized by the spin-dependent factor (cf. Eq. [4])

$$F_{\mathrm{ex}}^{\pm 1/2} = \frac{1}{9}\left\{\frac{2}{(2I+1)} + \frac{(2I+1)}{2} + \frac{(2I+1)^3}{32}\right\}, \quad [33]$$

where the labels "ex" and "$\pm 1/2$" refer to the fact that only the central levels are excited and spin exchange among the central levels is still allowed. Inserting spin quantum numbers, I, we find the values given in the first row of Table 2. Comparison with Table 1 shows that the reduced second moment for the *free-induction decay* describes very well the $\pi/2$—π spin-echo decay envelope for the selectively excited central transition.

We now suppose that the resonance frequencies of the *central* transitions of two neighboring I spins are different. This might be caused by very different quadrupolar couplings, or by chemical-shift interactions. In this case the spin exchange between the central levels of neighboring I spins can be completely suppressed. In order to describe the change in the spin-echo decay we again calculate a virtual (reduced) second moment of the free-induction decay. We sum up only matrix elements of the homonuclear dipolar interaction involving the central levels, $m = \pm 1/2$; however, we also discard all matrix elements responsible for the spin exchange. The result is that for spins with $m = \pm 1/2$, only the diagonal part of the homonuclear dipolar interaction contributes to the second moment. For the reduced second moment, we find that the spin-dependent factor is

$$F_{\mathrm{nex}}^{\pm 1/2} = \frac{2}{9(2I+1)}. \quad [34]$$

Inserting spin quantum numbers, we obtain the values given in the second row of Table 2. Comparison of Eq. [34] with Eq. [33] (Table 2) shows that the total suppression of spin exchange among the central levels causes a large decrease in the corresponding second moment. We now use these results to describe the influence of an additional heteronuclear dipolar interaction on the spin-echo decay of the central transition.

Homonuclear and heteronuclear dipolar interactions. If, in addition to a homonuclear dipolar interaction, a heteronuclear coupling is present, an exact calculation of the spin-echo decay is very complicated. The nonresonant S-spin system is responsible for two main effects. First, by influencing the resonance frequency of the I spin (IS interaction), which causes line broadening, it suppresses the spin flipping between like nuclei, and thus the spin-echo decay is slowed down. Second, spin flipping between the S spins (SS interaction) will decrease the phase coherence in the I-spin system, which tends to destroy the formation of the spin echo. In order to describe the spin-echo decay for two coupled spin systems quantitatively, we make the assumption that the above-mentioned processes can be approximated by the corresponding second moments, $M_{2\mathrm{F}}^{\mathrm{II}}$, $M_{2\mathrm{F}}^{\mathrm{IS}}$, $M_{2\mathrm{F}}^{\mathrm{SS}}$, $M_{2\mathrm{F}}^{\mathrm{SI}}$, higher-order moments being neglected. As we mentioned above, the spin-echo decay for a purely homonuclear dipolar interaction is well described by the reduced second moment, where we take only the central levels into account (Tables 1 and 2). Upon introducing an additional heteronuclear coupling, the spin flipping in the I system vanishes completely, since the secular part of the homonuclear interaction no longer contains x and y components of the angular momentum operators (which leads to further truncation of $\mathcal{H}_{\mathrm{D}}$). Thus, the second moment of the spin-echo decay for the I-spin system [denoted as $M_{2\mathrm{E}}(I)$] in the presence of a sufficiently strong heteronuclear dipolar coupling decreases drastically, to the value

$$M_{2\mathrm{E}}(I) = M_{2\mathrm{F}}^{\mathrm{II}} \frac{F_{\mathrm{nex}}^{\pm 1/2}(I)}{F_{\mathrm{L}}(I)}. \quad [35]$$

If a heteronuclear coupling causes this drastic decrease, the coupling to the S-spin system, $M_{2\mathrm{F}}^{\mathrm{IS}}$, will in general be larger than $M_{2\mathrm{E}}(I)$. So, the two spin systems appear to be strongly coupled, and we approximate the influence of the S-spin system by assuming an echo intensity, $E(2\Delta)$, having the form

$$E(2\Delta) = \exp\left\{-\frac{M_{2\mathrm{E}}(I)}{2}(2\Delta)^2\right\} \times \exp\left\{-\frac{M_{2\mathrm{E}}(S)}{2}(2\Delta)^2\right\}, \quad [36]$$

TABLE 2

Ratio of the Reduced Second Moments to the Ordinary Second Moment of the Homonuclear Dipolar Coupling, for Different Spin Quantum Numbers, I

	$I = 3/2$	$I = 5/2$	$I = 7/2$	$I = 9/2$
$F_{\mathrm{ex}}^{\pm 1/2}/F_{\mathrm{L}}$	4/9	41/107	324/881	729/1961
$F_{\mathrm{nex}}^{\pm 1/2}/F_{\mathrm{L}}$	4/81	4/321	4/881	4/1961

Note. $F_{\mathrm{ex}}^{\pm 1/2}$ represents the sum of matrix elements of the dipolar Hamiltonian which involve only the central levels ($m = \pm 1/2$), but still allowing for spin exchange among the central transitions. $F_{\mathrm{nex}}^{\pm 1/2}$ indicates no exchange was allowed for during collection of the appropriate matrix elements, $m, m' = \pm 1/2$. From Eqs. [33] and [34] in the text.

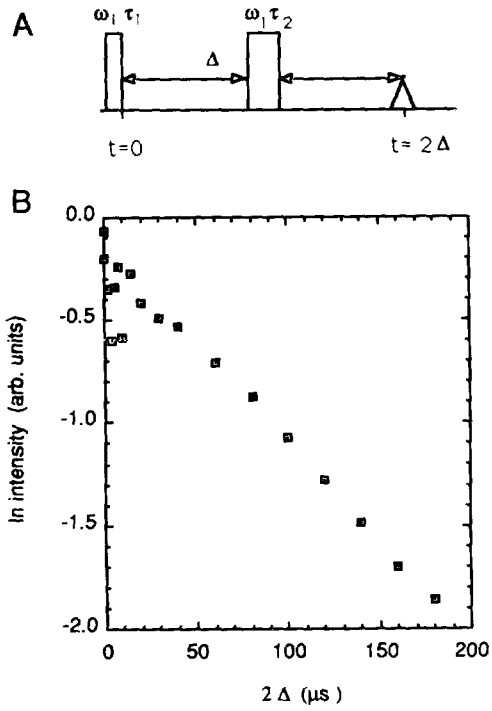

FIG. 1. (A) Spin-echo pulse sequence used to record T_{2E} data. (B) Semilogarithmic spin-echo decay data obtained on α-Al_2O_3 (corundum) single crystal following a selective $\pi/2$ (2.4 μs)—selective π (4.8 μs) pulse pair, at 11.7 T. The crystal was aligned (c axis parallel to the static magnetic field) by measuring the frequency difference between the central and satellite transitions.

where $M_{2E}(I)$ refers to the second moment of the spin-echo decay, Eq. [35], in the I system, if no spin flipping occured in the S-spin system.

If both I- and S-spin systems are subjected to strong quadrupolar coupling, $M_{2E}(S)$ must be calculated from Eq. [35]. In the special case that the S spins have a vanishing quadrupolar coupling (spin exchange is not restricted), or $S = 1/2$, $M_{2E}(S)$ is given by van Vleck's formula for the S-spin homonuclear dipolar interaction, Eqs. [2] and [3].

The $1/e$ decay time deduced from Eq. [36] for a Gaussian decay of the spin echo now becomes

$$T_{2E} = \sqrt{2/[M_{2E}(I) + M_{2E}(S)]}. \qquad [37]$$

If the heteronuclear dipolar coupling is negligible, $M_{2E}(S) = 0$ in Eq. [37], then $M_{2E}(I)$ can be replaced by M_{2E}, given by Eqs. [25] and [26], and we obtain

$$T_{2E} = \sqrt{2/M_{2E}}. \qquad [38]$$

RESULTS AND DISCUSSION

Before we compare the theoretical predictions with the experimental results obtained for different nuclei in a variety of inorganic solids, we will briefly consider the effects of selective/nonselective excitation. A not entirely selective excitation can severely alter the results of spin-echo experiments, and this topic is addressed in a forthcoming paper. We give a qualitative description of these results here, since they represent one means of determining selectivity.

Excitation aspects. We show in Fig. 1B the spin-echo amplitude as a function of pulse spacing (2Δ) for nonselective excitation of the ^{27}Al spins in a ruby (Cr^{3+}-doped corundum, α-Al_2O_3) single crystal aligned with its c axis parallel to the static magnetic field. While the long-time echo-decay behavior appears monotonic, there are clearly short-time oscillations, which are caused by components of the magnetization precessing at the quadrupole frequency. The origin of these oscillations has been described previously (*14*) and can be used to measure reduced powder spectra for half-integer-spin quadrupolar nuclei.

In Fig. 2 it can be seen that for a Hahn-echo sequence on corundum powder, the T_{2E} values are hardly influenced by the RF excitation, but the intensity of the spin-echo for $\Delta = 0$ can be much smaller than the intensity of the free-induction decay observed after a single $\pi/2$ pulse. This decrease of the spin-echo amplitude with increasing nonselectivity of excitation is typical for the in-phase $\pi/2$—π pulse sequence: If the excitation affects also the satellite transitions, the effect of the second pulse for refocusing the central transition decreases. It also creates an ordinary free-induction decay due

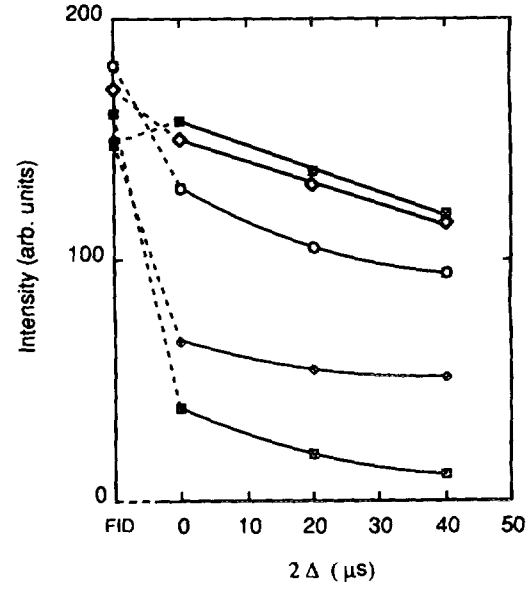

FIG.2. Comparison between the intensity of the 130.2 MHz (11.7 T) ^{27}Al free-induction decays in α-Al_2O_3 (corundum powder) and the echo intensity for a spin-echo sequence, using selective $\pi/2$ pulse widths of □, 2 μs; ◆, 4 μs; ○, 8 μs; ◇, 12 μs; and ■, 25 μs. The recycle time was 30 seconds. The five intensities on the left (FID) represent the observed free-induction decay amplitudes following a $\pi/2$ selective pulse at each RF field strength.

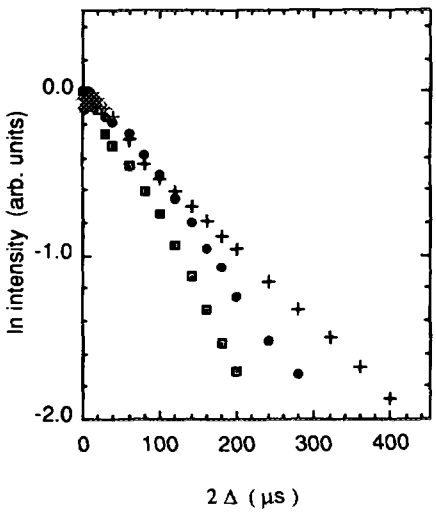

FIG. 3. Semilogarithmic spin-echo decays for the 130.2 MHz (11.7 T) ^{27}Al 1/2, −1/2 (□), −1/2, −3/2 (●), and −3/2, −5/2 (+) transitions in a single crystal of ruby; 15 μs $\pi/2$ and 30 μs π pulses were used. The recycle time was 1 s. The crystal was aligned by measuring the frequency difference between the central and satellite transitions.

to spins not affected by the first pulse. This free-induction decay, especially its slowly decaying central transition component, is superimposed on the spin echo at a time $t = 2\Delta$. Since the second pulse represents a weak pulse for the satellite transitions, the second free-induction decay is in-phase with the second pulse. Thus, for pulse distances smaller than the decay of the second component, the spin-echo amplitude is even more suppressed.

Now, the difference between the in-phase $\pi/2$—π sequence and the 90° phase-shifted $\pi/2$—π pulse sequence is given by this second free-induction decay. For the 90° phase-shifted sequence, the free-induction decay caused by the second pulse is 90° shifted with respect to the spin echo. Thus, the experimentally observed signal, at $t = 2\Delta$, appears to be phase shifted compared with the one-pulse free-induction decay. However, the amplitude of the experimentally observed echo is not affected as much as that for the in-phase pulse sequence. Since for both pulse sequences the spin-echo decay depends on the bandwidth of excitation, it is critically important to prove selective excitation if spin-echo experiments are to be interpretable. Selective excitation can be proven by recording the intensity of the free induction as a function of the pulse duration (5), or by utilizing the above-mentioned effects on the spin-echo phase and amplitude.

Spin-echo results. Experiments on a ruby *single crystal* revealed a spin–lattice relaxation time, T_1, of $\approx$100 ms. The linewidths of the transition were 8 kHz for the central and 9 kHz for each satellite transition. The theoretical values for Gaussian lines are 7.3, 6.9, and 6.0 kHz, assuming a second moment of the central line (Eqs. [4], [28], and [30]) of $3.75 \times 10^8\ s^{-2}$ (*15*). The deviation of the experimental values from the theoretical ones, as well as the short T_1, are presumably due in part to increased doping of the ruby crystal with paramagnetic centers. Figure 3 shows the spin-echo decay envelopes for a crystal whose c axis was parallel to the static field. For a Gaussian decay, the $1/e$ decay time, T_{2E}, of the echo train follows from the second moments, M_{2E} (Eqs. [38], [25], and [26]). The theoretical values, assuming an M_{2F} (Eq. [2]) of $3.75 \times 10^8\ s^{-2}$, are

$$T_{2E}^{(0)} = 112\ \mu s \quad \text{(central line)},$$

$$T_{2E}^{(1)} = 115\ \mu s \quad \text{(first satellite)},$$

$$T_{2E}^{(2)} = 119\ \mu s \quad \text{(second satellite)}.$$

We obtain good agreement for the central transition $T_{2E}^{(0)} = 130 \pm 10\ \mu s$, but the difference between theory and the experimental values of $T_{2E}^{(1)} = 160 \pm 15\ \mu s$ and $T_{2E}^{(2)} = 220 \pm 20\ \mu s$ for the satellite transitions shows the great sensitivity of echo measurements on satellite lines to lattice defects. Figure 4A shows the echo-decay result for corundum powder. The measured T_{2E} is given by the homonuclear dipolar interaction, as for the single-crystal experiments, and we find $T_{2E} = 140 \pm 20\ \mu s$, in accord with the single-crystal result.

The spin-echo decays of three different types of AlN powders are shown in Fig. 4B. The static spectrum of sample 1 has a width of 6.6 kHz and a T_1 of about 5 s, while the linewidths and T_1 values for samples 2 and 3 are 8.2 kHz, 1 s and 14 kHz, 1 s, respectively. Using the theoretical M_{2F} of $2.1 \times 10^8\ s^{-2}$ (*7*), we estimate that T_{2E} for the Gaussian spin-echo decay should be 150 μs (assuming a negligible influence of the ^{14}N nuclei). The experimental results are

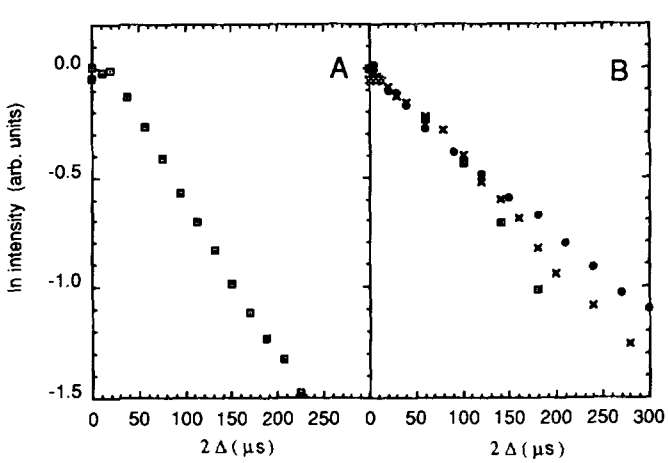

FIG. 4. Spin-echo decays for ^{27}Al at 130.2 MHz (11.7 T) in (A) powdered corundum and (B) several AlN powders. For corundum, the selective $\pi/2$ pulse width was 27.5 μs and the selective π pulse width was 55 μs. For AlN, the selective $\pi/2$ pulse width was 16.5 μs and the selective π pulse width was 33 μs: □, AlN(1); ●, AlN(2); and ×, AlN(3).

180 ± 20 μs, 210 ± 20 μs and 260 ± 25 μs. The samples having the largest linewidths and shortest T_1 values are those which might be supposed to be the least homogeneous (both chemically and crystallographically), resulting in a lengthening of T_{2E}, because of suppression of spin-flip processes for the central transition.

For γ-Al_2O_3, the spin-echo decay shown in Fig. 5 reveals a T_{2E} of about 580 ± 30 μs ($T_1 \approx 50$ ms). γ-Al_2O_3, which is thought to have a defect spinel structure, has two different Al nuclei which can be resolved in high-resolution "magic-angle" sample-spinning spectra (*16*). For each unit cell (32 oxygen atoms) we have 8 tetrahedrally coordinated Al atoms and 13.33 octahedrally coordinated Al atoms. To estimate the upper limit for T_{2E} of γ-Al_2O_3, we need to consider the two types of Al nuclei as an IS system; i.e., each species is mutually coupled by a *heteronuclear* dipolar interaction. Since single crystal X-ray diffraction data on γ-Al_2O_3 are not available, for an estimate of the strength of this interaction we may use the density of γ-Al_2O_3 compared to that of α-Al_2O_3. We then obtain ratios of about 1.1, 3.0, and 1.8 for the total number of Al atoms and tetrahedrally and octahedrally coordinated Al atoms, respectively (*17*). With the known M_{2F}^{II} for α-Al_2O_3 and Eqs. [34] and [38] we can then estimate a T_{2E} of about 730 μs for each site. From the experimental observation that the separation between the two Al resonances in γ-Al_2O_3 is not complete, it is clear that the observed T_{2E} should be somewhat smaller than this value, but much longer than that for α-Al_2O_3. Thus, the experimental value of about 580 μs can be easily understood.

In the zeolite Linde A, calculation of the second moment for the homonuclear Al–Al interaction, considering the 21 nearest Al neighbors, gives $M_2 \sim 8.3 \times 10^6$ s^{-2}. Assuming a Gaussian spin-echo decay and a vanishing heteronuclear coupling to the Na and H nuclei (due to fast particle reorientation), one expects $T_{2E} = 750$ μs. Comparison with the experimental T_{2E}, 730 ± 50 μs, shown in Fig. 6A gives good agreement ($T_1 \approx 1$ ms), supporting the assumption of only like Al atoms in the NaA framework. The spin-echo decay for a hydrated $Na_{3.6}Ca_{4.2}A$ zeolite ($T_1 \approx 1$ ms) shows the same T_{2E}, indicating that the single-site symmetry is not greatly disturbed by cation substitution, at least in a hydrated sample. For the hydrated zeolite NaA at −130°C, we measured a T_{2E} of 550 ± 30 μs ($T_1 \approx 30$ ms). Since there is not thought to be any large structural change in this temperature range, we believe that at low temperatures the ^{27}Al–^{1}H dipolar interaction contributes to the linewidth of the ^{27}Al resonance (*18*), and most likely the stronger H–H dipolar interaction shortens the ^{27}Al decay from that observed at room temperature. The ^{23}Na and ^{27}Al resonances in the natural mineral albite ($NaAlSi_3O_8$; $T_1 \approx 6$ s for both nuclei) showed linewidths of about 6.5 and 4.5 kHz, respectively. The second moments (18 neighbors) are 3.2×10^6 and 5.3×10^6 s^{-2} for the Na–Na and Al–Al couplings, respectively. The theoretical prediction (Eqs. [36] and [37]) from these values yields T_{2E} values of about 3.0 ms. The experimental results are 2.7 ± 0.2 ms, for both decays, as shown in Fig. 6B.

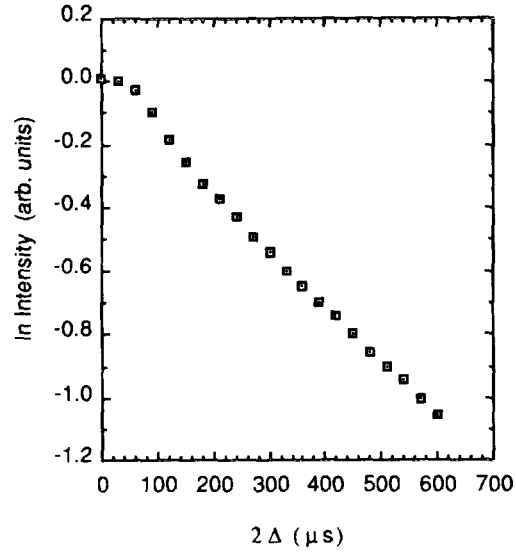

FIG. 5. Spin-echo decay for ^{27}Al in γ-Al_2O_3 at 11.7 T. The selective $\pi/2$ pulse width was 9.5 μs, and the selective π pulse width was 19 μs. The echo decay represents contributions from both tetrahedral and octahedral sites.

In $NaNO_3$, the ^{23}Na resonance ($T_1 \approx 5$ s) was recorded at 11.7 T and revealed a symmetric line of 1.6 kHz width. The second moment of the Na–Na interaction (for the 24 nearest neighbors) is 12×10^6 s^{-2}. The ^{14}N nuclei are thought to have a negligible influence on the Na resonance, due to their small gyromagnetic ratio and relatively long distance to Na. From the second moment, we calculate (by using Eq. [38]) an echo decay $T_{2E} = 600$ μs. Comparison with the experimental value of 650 ± 50 μs obtained from Fig. 7A suggests that the slight discrepancy could be due to the influence of the ^{14}N nuclei, which, due to a weak N–N interaction, tend to lengthen the spin-echo decay somewhat, although the difference is within our experimental error.

In $KNbO_3$, the ^{93}Nb resonance ($T_1 \approx 350$ ms) showed a linewidth of about 23 kHz, mainly due to second-order quadrupolar effects. The potassium nuclear spin has essentially no influence on the behavior of the Nb spins, due to its very low gyromagnetic ratio (the K–K second moment is about 1.1×10^4 s^{-2}). Taking into account the 18 Nb nearest neighbors, the second moment of 5.6×10^7 s^{-2} predicts a T_{2E} of about 280 μs, which is in quite good agreement with the observed value of 220 ± 20 μs (Fig. 7B).

In $NaNbO_3$, the observed linewidths for ^{93}Nb ($T_1 \approx 350$ ms) and ^{23}Na ($T_1 \approx 18$ s) resonances were about 16 and 5.5 kHz, respectively. The second moments of the Na–Na and the Nb–Nb interactions (again considering 18 near neighbors) are 1.36×10^7 and 6.53×10^7 s^{-2}, respectively.

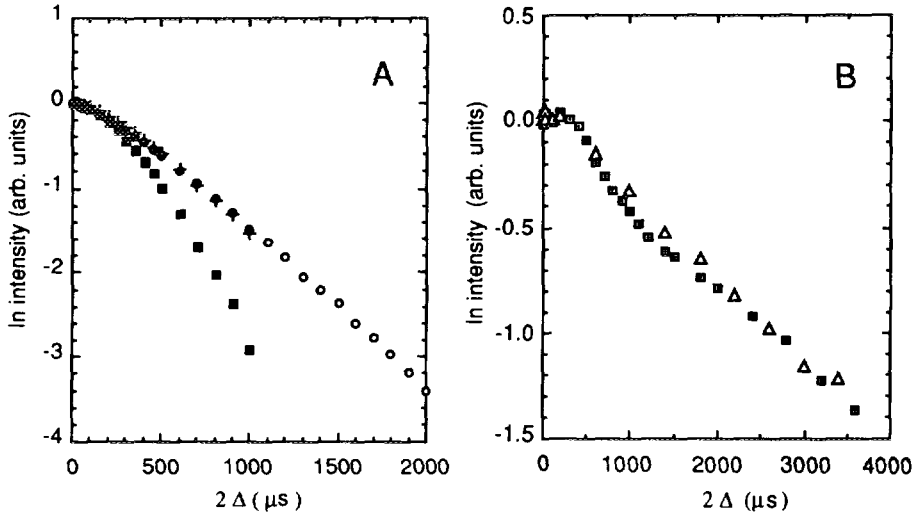

FIG. 6. Spin-echo decay data for zeolites and albite. (A) Static 93.8 MHz (8.45 T) ^{27}Al spin-echo decay behavior for fully hydrated zeolites NaA (○) and $Na_{3.6}Ca_{4.2}A$ (+) at room temperature and NaA (■) at −130°C, using selective $\pi/2$ pulse widths of 38 μs and selective π pulse widths of 76 μs. (B) Static 130.2 MHz (11.7 T) ^{27}Al (□) and 132.2 MHz ^{23}Na (△) spin-echo decay results on the mineral albite, using $\pi/2$ pulse widths of 7.5 μs and selective π pulse widths of 15 μs.

From Eq. [37] we estimate an echo decay of about 1.6 ms. Comparison of this value with the experimental result of T_{2E} = 1.2 ms for the ^{23}Na resonance and 1.3 ms for ^{93}Nb resonance, as shown in Fig. 7, reveals a small discrepancy, which is probably not due to the finite lattice sum for the second moments, but rather to incomplete suppression of spin flipping in the Nb central transition.

For $LiNbO_3$, we measured only the Nb resonance (the Li signal was very broad), which revealed a linewidth of about 25 kHz ($T_1 \approx 350$ ms). The second moments, including the 18 nearest neighbors, are 7.9×10^7 and 8.2×10^7 s^{-2} for the Li–Li and Nb–Nb interactions, respectively. Because of the much larger Li gyromagnetic ratio (194.3 MHz at 11.7 T), the Li–Li and Li–Nb interactions are stronger than those in $NaNbO_3$ and tend to shorten the spin-echo decay. Application of Eq. [37] predicts a T_{2E} for the Nb nuclei of about 670 μs, while experimentally we find $T_{2E} = 650 \pm 60$ μs (Fig. 7B).

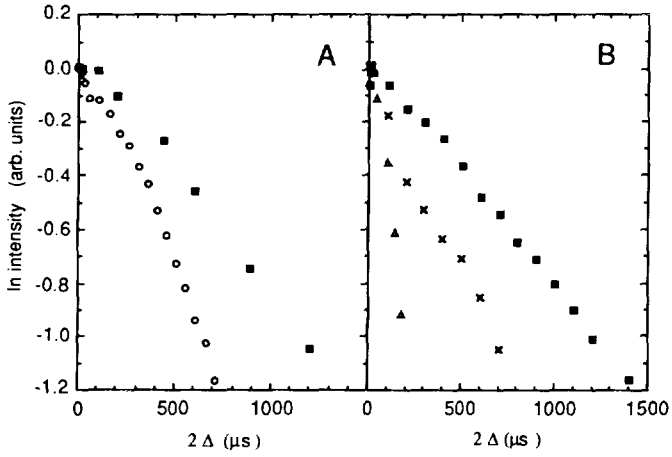

FIG. 7. Hahn-echo decay data for some niobates and sodium nitrate. (A) Static 132.2 MHz (11.7 T) ^{23}Na spin-echo decay behavior for $NaNbO_3$ (■) and $NaNO_3$ (○), using a selective $\pi/2$ pulse width of 7.5 μs and a selective π pulse width of 15 μs for $NaNbO_3$ and 18 and 36 μs for $NaNO_3$. (B) Static 122.2 MHz (11.7 T) ^{93}Nb Hahn-echo decay behavior for $KNbO_3$ (△), $LiNbO_3$ (×), and $NaNbO_3$ (■), using selective $\pi/2$ pulse widths of 5 μs and selective π pulse widths of 10 μs.

The results that we have presented above show, with few exceptions, that the spin-echo decay behavior of nonintegral-spin quadrupolar nuclei in a wide variety of inorganic solids—ranging from highly ordered ruby single crystals to random powders of zeolites and aluminas—can be quantitatively explained in terms of homonuclear and heteronuclear dipolar interactions which are modulated by various sample-dependent properties, such as the presence of chemically shifted resonances in γ-Al_2O_3, the freezing of zeolitic water in the zeolite Linde A, or lattice imperfections. A detailed analysis of the spin-echo decay rate, T_{2E}, provides a potentially important probe of local structure, which complements existing chemical-shift and electric field gradient tensor information.

REFERENCES

1. E. Oldfield and R. J. Kirkpatrick, *Science* **227**, 1537 (1985).
2. J. Haase, K. D. Park, K. Guo, H. K. C. Timken, and E. Oldfield, *J. Phys. Chem.* **95**, 6996 (1991).
3. D. Y. Han and H. Kessemeier, *Phys. Rev. Lett.* **67**, 346 (1991).
4. J. Dolinsek, *J. Magn. Reson.* **92**, 312 (1991).

5. D. Fenzke, D. Freude, T. Fröhlich, and J. Haase, *Chem. Phys. Lett.* **111,** 171 (1984).
6. D. I. Hoult and R. E. Richards, *Proc. R. Soc. London Ser. A* **344,** 311 (1975).
7. J. Haase, D. Freude, T. Fröhlich, G. Himpel, F. Kerbe, E. Lippmaa, H. Pfeifer, P. Sarv, H. Schäfer, and B. Seiffert, *Chem. Phys. Lett.* **156,** 328 (1989).
8. M. H. Cohen and F. Reif, *Solid State Phys.* **5,** 321 (1957).
9. K. Kambe and J. F. Ollom, *J. Phys. Soc. Jpn.* **11,** 50 (1956).
10. M. Mansfield, *Phys. Rev.* **137,** A961 (1965).
11. A. Abragam, "Principles of Nuclear Magnetism," Oxford Univ. Press, Oxford, 1961.
12. M. Mehring, "Principles of High Resolution NMR in Solids," Springer-Verlag, Berlin/Heidelberg/New York, 1983.
13. U. Haeberlen, "High Resolution NMR in Solids, Selective Averaging," Academic Press, New York/San Francisco/London, 1976.
14. J. Haase and H. Pfeifer, *J. Magn. Reson.* **86,** 217 (1990).
15. C. M. Brodbeck, S. Lee, and H. H. Niebuhr, *Phys. Rev. B* **10,** 844 (1974).
16. V. M. Mastikhin, O. P. Krivoruchko, B. P. Zolotovskii, and R. A. Byyanov, *React. Kinet. Catal. Lett.* **18,** 117 (1981).
17. Landolt-Börnstein, "Numerical Data and Functional Relationships in Science and Technology," New Series, New York, 1975.
18. H. K. C. Timken, Thesis, University of Illinois at Urbana-Champaign, 1987.